

# FY17 Status Report on Testing Supporting the Inclusion of Grade 91 Steel as an Acceptable Material for Application of the EPP Methodology



Yanli Wang  
Mark C. Messner  
T.-L. Sham

**August 25, 2017**

**Approved for public release.  
Distribution is unlimited.**

## DOCUMENT AVAILABILITY

Reports produced after January 1, 1996, are generally available free via US Department of Energy (DOE) SciTech Connect.

**Website** <http://www.osti.gov/scitech/>

Reports produced before January 1, 1996, may be purchased by members of the public from the following source:

National Technical Information Service  
5285 Port Royal Road  
Springfield, VA 22161  
**Telephone** 703-605-6000 (1-800-553-6847)  
**TDD** 703-487-4639  
**Fax** 703-605-6900  
**E-mail** [info@ntis.gov](mailto:info@ntis.gov)  
**Website** <http://www.ntis.gov/help/ordermethods.aspx>

Reports are available to DOE employees, DOE contractors, Energy Technology Data Exchange representatives, and International Nuclear Information System representatives from the following source:

Office of Scientific and Technical Information  
PO Box 62  
Oak Ridge, TN 37831  
**Telephone** 865-576-8401  
**Fax** 865-576-5728  
**E-mail** [reports@osti.gov](mailto:reports@osti.gov)  
**Website** <http://www.osti.gov/contact.html>

This report was prepared as an account of work sponsored by an agency of the United States Government. Neither the United States Government nor any agency thereof, nor any of their employees, makes any warranty, express or implied, or assumes any legal liability or responsibility for the accuracy, completeness, or usefulness of any information, apparatus, product, or process disclosed, or represents that its use would not infringe privately owned rights. Reference herein to any specific commercial product, process, or service by trade name, trademark, manufacturer, or otherwise, does not necessarily constitute or imply its endorsement, recommendation, or favoring by the United States Government or any agency thereof. The views and opinions of authors expressed herein do not necessarily state or reflect those of the United States Government or any agency thereof.

Materials Science and Technology Division

**FY17 STATUS REPORT ON TESTING SUPPORTING THE INCLUSION OF  
GRADE 91 STEEL AS AN ACCEPTABLE MATERIAL FOR  
APPLICATION OF THE EPP METHODOLOGY**

Yanli Wang, Mark C. Messner\* and T.-L. Sham\*

\*Argonne National Laboratory

August 25, 2017

Prepared by  
OAK RIDGE NATIONAL LABORATORY  
Oak Ridge, TN 37831-6283  
managed by  
UT-BATTELLE, LLC  
for the  
US DEPARTMENT OF ENERGY  
under contract DE-AC05-00OR22725



# CONTENTS

LIST OF FIGURES .....	ii
LIST OF TABLES .....	iii
ACRONYMS .....	iv
ACKNOWLEDGMENTS .....	v
ABSTRACT .....	vi
1. BACKGROUND .....	1
1.1 SMT Key Feature Testing Approach .....	1
1.2 Two-bar Thermal Ratcheting Key Feature Testing Approach .....	2
2. EXPERIMENTAL DETAILS .....	3
2.1 Material .....	3
2.2 Specimens and Experiments .....	5
2.2.1 Specimen geometries .....	5
2.2.2 Key feature mechanical testing .....	6
2.2.3 Mechanical tests to support viscoplastic material model development .....	9
3. RESULTS AND DISCUSSIONS .....	12
3.1 Results from Key Feature Mechanical Testing .....	12
3.1.1 Type 1 SMT Testing .....	12
3.1.2 Two-bar thermal ratcheting test results .....	13
3.2 Results from Mechanical Tests in Support of Viscoplastic Material Model Development .....	16
3.2.1 Cyclic stress-strain curves .....	16
3.2.2 Sequential creep and strain controlled cycling .....	19
3.2.3 Effect of prior strain controlled cycling on strain rate sensitivity .....	21
3.2.4 Thermomechanical fatigue .....	22
4. SUMMARY .....	24
REFERENCES .....	25

## LIST OF FIGURES

Fig. 1. Definition of elastic follow-up.....	2
Fig. 2. Pressurized cylinder with radial thermal gradient represented by a two-bar model.....	2
Fig. 3. Gr.91 plate with heat number 30176. ....	3
Fig. 4. Back-scatter image of the Gr. 91 plate (heat 30176) after heat treatment. ....	4
Fig. 5. Microstructure of the F91 bar material at center line. ....	4
Fig. 6. Vickers microhardness of the F91 bar material. ....	5
Fig. 7. Standard creep-fatigue specimen geometry. Units are in inches. ....	5
Fig. 8. Type 1 SMT solid bar specimen geometry. Units are in inches. ....	6
Fig. 9. Applied end-displacement profile for one cycle of SMT creep-fatigue testing compression hold .....	7
Fig. 10. Two-bar thermal cycle. ....	7
Fig. 11. Schematics of the combined creep/fatigue experiments.....	10
Fig. 12. Test results for test #39-Type 1 SMT on F91 (heat 307333) at 650° C. ....	13
Fig. 13. An example of the thermal profile with 10 mins. time delay. ....	14
Fig. 14. Cyclic stress-strain evaluation of Gr. 91 (heat 30176) at 21° C. Black lines are the first cycles and red lines are the last cycles.....	17
Fig. 15. Cyclic stress-strain evaluation of Gr. 91 (heat 30176) at 260° C. Black lines are the first cycles and red lines are the last cycles.....	17
Fig. 16. Cyclic stress-strain evaluation of Gr. 91 (heat 30176) at 371° C. Black lines are the first cycles and red lines are the last cycles.....	17
Fig. 17. Cyclic stress-strain evaluation of Gr. 91 (heat 30176) at 427° C. Black lines are the first cycles and red lines are the last cycles.....	18
Fig. 18. Cyclic stress-strain evaluation of Gr. 91 (heat 30176) at 482° C. Black lines are the first cycles and red lines are the last cycles.....	18
Fig. 19. Cyclic stress-strain evaluation of Gr. 91 (heat 30176) at 538° C. Black lines are the first cycles and red lines are the last cycles.....	18
Fig. 20. Cyclic stress-strain evaluation of Gr. 91 (heat 30176) at 566° C. Black lines are the first cycles and red lines are the last cycles.....	19
Fig. 22. Combined creep-fatigue test on Gr. 91 (heat 30176) at 600° C. ....	20
Fig. 23. Combined creep-fatigue test on Gr. 91 (heat 30176) at 550° C. ....	21
Fig. 24. Effect of cyclic softening on strain rate sensitivity.....	22
Fig. 25. Thermal expansion measurement (Gr. 91 heat 37016).....	23
Fig. 26. Thermo-mechanical fatigue at temperature range of 150 to 650° C. ....	23

**LIST OF TABLES**

Table 1. Chemical compositions of Gr. 91 plate with heat number 30176 (weight %)..... 3  
Table 2. Chemical compositions of F91 bar material with heat number 307333 (weight %)..... 4  
Table 3. Parameters of the two-bar experiment and EPP analysis..... 9  
Table 4. Cyclic stress-strain evaluation of Gr. 91 (heat 30176)..... 9  
Table 5. Test parameters for combined creep and fatigue experiment on Gr. 91 (heat 30176)..... 10  
Table 6. Test parameters for rate jump experiment on Gr. 91 (heat 30176)..... 11  
Table 7. Test parameters for thermomechanical experiment on Gr. 91 (heat 30176)..... 11  
Table 8. Summary of the SMT creep-fatigue results ..... 12  
Table 9. Summary of the two-bar thermal ratcheting experiments on Gr. 91 (heat 30176) for  
temperature range of 350 to 650° C..... 15  
Table 10. Two-bar thermal ratcheting results on Gr. 91 (heat 30176) with 350 hr extrapolation. .... 16  
Table 11. Effect of cyclic softening on strain rate sensitivity ..... 22

## ACRONYMS

ART	Advanced Reactor Technologies Program
ANL	Argonne National Laboratory
ASME	American Society of Mechanical Engineers
B&PV	Boiler and Pressure Vessel
DOE	Department of Energy
EPP	Elastic – Perfectly Plastic
ORNL	Oak Ridge National Laboratory
SMT	Simplified Model Test

## **ACKNOWLEDGMENTS**

The research was sponsored by the U.S. Department of Energy, under contract No. DE-AC05-00OR22725 with Oak Ridge National Laboratory (ORNL), managed and operated by UT-Battelle, LLC. Programmatic direction was provided by the Office of Advanced Reactor Technologies (ART) of the Office of Nuclear Energy (NE). We gratefully acknowledge the support provided by William Corwin of DOE-NE, ART Materials Technology Lead and Robert Hill of Argonne National Laboratory, ART Co-National Technical Director.

Technical support from Shane Hawkins of ORNL is acknowledged. The authors thank Robert Jetter of R.I. Jetter Consulting for discussions on the EPP and SMT design methodologies. The time spent by Lianshan Lin, Hong Wang and Edgar Lara-Curzio of ORNL in reviewing this report is greatly appreciated.

## ABSTRACT

This report summarizes the experiments performed in FY17 on Gr. 91 steels. The testing of Gr. 91 has technical significance because, currently, it is the only approved material for Class A construction that is strongly cyclic softening. Specific FY17 testing includes the following activities for Gr. 91 steel. First, two types of key feature testing have been initiated, including two-bar thermal ratcheting and Simplified Model Testing (SMT). The goal is to qualify the Elastic – Perfectly Plastic (EPP) design methodologies and to support incorporation of these rules for Gr. 91 into the ASME Division 5 Code. The preliminary SMT test results show that Gr. 91 is most damaging when tested with compression hold mode under the SMT creep fatigue testing condition. Two-bar thermal ratcheting test results at a temperature range between 350 to 650° C were compared with the EPP strain limits code case evaluation, and the results show that the EPP strain limits code case is conservative. The material information obtained from these key feature tests can also be used to verify its material model. Second, to provide experimental data in support of the viscoplastic material model development at Argonne National Laboratory, selective tests were performed to evaluate the effect of cyclic softening on strain rate sensitivity and creep rates. The results show the prior cyclic loading history decreases the strain rate sensitivity and increases creep rates. In addition, isothermal cyclic stress-strain curves were generated at six different temperatures, and a non-isothermal thermomechanical testing was also performed to provide data to calibrate the viscoplastic material model.

## 1. BACKGROUND

Simplified design rules based on using elastic analysis results to satisfy deformation limits for Class A components are provided in Division 5 Appendix HBB-T of ASME's Boiler and Pressure Vessel Code. These bounding methods were established as conservative screening tools, with the expectation that inelastic analyses would sometimes be required. The technical basis of the simplified design methods was developed with the tacit assumption that plastic and creep deformation are uncoupled. When such conditions are not met, e.g., at higher temperatures, the technical basis of the simplified design rules is no longer valid.

The Elastic – Perfectly Plastic (EPP) methods were developed as bounding methods for strain limits and creep-fatigue evaluations to address this deficiency. The EPP methods are valid for the full range of allowable temperatures, even when plasticity and creep are coupled. Furthermore, they are tailored to modern finite element analysis tools, with no stress classification and no restrictions on geometry or loading, and also account for redundant load paths. Currently, the EPP strain limits and creep-fatigue evaluation procedures are approved for 304H and 316H stainless steels through the ASME Section III Division 5 code cases, N-861 and N-862, respectively.

Grade 91 steel is currently an approved material for Class A construction in ASME Section III Division 5, Subsection HB, Subpart B. Qualification of Grade 91 steel for the EPP strain limits and creep-fatigue evaluations is a high priority R&D item of the ASME Code committee responsible for Division 5. Development of an inelastic analysis method for Grade 91 steel is also a Code committee high priority item. Experimental investigations are designed to support these two tasks.

In FY17, two types of key feature test experiments used to qualify the EPP methods for 304H and 316H stainless steels have been initiated to support their qualification for Grade 91 steel. The first key feature test approach employs the so-called Simplified Model Test (SMT), which is a test article that is sized to incorporate the elastic follow-up effects that are representative of actual components. The second key feature testing method corresponds to two-bar thermal ratchet experiments.

Experimental efforts were also initiated in FY17 to generate data to support a parallel effort at the Argonne National Laboratory (ANL) on the development of a viscoplastic material model for Grade 91. The types of tests conducted in FY17 included the generation of cyclic stress-strain curves, the sequential creep and strain-controlled cycling tests, strain rate jump tests on materials that have been pre-conditioned under strain-controlled cycling, and thermomechanical fatigue.

The qualification of the EPP methods and the development of the inelastic analysis method for Grade 91 steel have technical significance because this steel is the only currently approved material for Division 5 Class A construction that is strongly cyclic softening.

### 1.1 SMT KEY FEATURE TESTING APPROACH

The basic concept of the SMT methodology was to provide an alternative approach to evaluation of creep-fatigue damage of actual structures with a suitably sized specimen that models the actual structural stress and strain redistribution (Jetter, 1998, Wang, et. al., 2015). The component design is represented by a stepped cylinder with a stress concentration at the shoulder fillet radius. The component has a global elastic follow-up,  $q_n$ , which is due to the interaction between the two cylindrical sections, and a local follow-up,  $q_L$ , which is due to the local stress concentration. The effect of elastic follow-up on the stress-

strain curve is shown in Fig. 1. The elastic follow-up factor,  $q$ , is defined as the strain ratio of  $\epsilon_{0-2}/\epsilon_{0-1}$ . Note that a follow-up of  $q=1.0$  corresponds to pure stress relaxation.

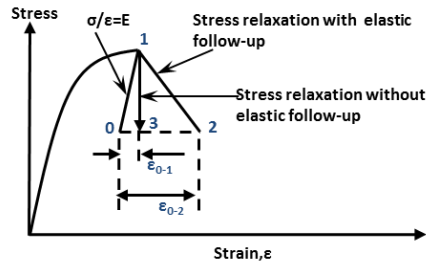


**Fig. 1. Definition of elastic follow-up.**

For this application, the SMT results provide both a component representation that can be used to verify the conservatism of the EPP creep-fatigue evaluation methodology as well as data that can be used to verify the constitutive equations developed for inelastic analysis. The SMT geometry has the advantage that key parameters can be directly measured.

## 1.2 TWO-BAR THERMAL RACHETING KEY FEATURE TESTING APPROACH

The experimental control logic used is similar to what was previously reported by Swindeman et al. (1982) and is explained in detail in Wang et al. (2013, 2015, 2016). In this method, two coupled servo-hydraulic machines are used to implement two bars of equal lengths in a parallel testing condition and the control system forces equal strains in the two specimens, yet allows the applied total load to be constant. The two bars are installed in two, coupled, servo-hydraulic machines with machine #1 under strain control and machine #2 under load control. The strain signals measured by the extensometer on Bar 2 are fed into machine #1 as the command signal for strain control of Bar 1. This control logic ensures an equal amount of deformation for the two bars at all times. The driving force for the specimens to experience deformation is the constant total load of the two bars and the cyclic temperature history applied to each bar. A two-bar model is a simplified analysis of a vessel under a combination of a constant, primary pressure load and a secondary, alternating thermal cycle. The two bars represent two extreme material fibers (schematically shown in Fig. 2).

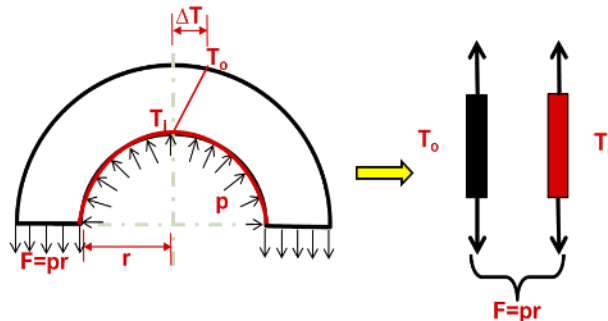


**Fig. 2. Pressurized cylinder with radial thermal gradient represented by a two-bar model.**

## 2. EXPERIMENTAL DETAILS

### 2.1 MATERIAL

Two product forms of Grade 91 materials were used in this research, i.e., the Gr. 91 plate (heat 30176) and SA-182, F91 forged bar (heat 307333). The Gr. 91 plate (heat 30176) is a historical material at ORNL, manufactured by Carpenter Technology Corporation in the early 1980s. ORNL technical report, ORNL-6303, has documented the chemical composition of this plate which is also listed in Table 1 below. It is noted that the silicon content is 0.11%, lower than the ASME SA-387 specification of 0.2-0.5%. This plate was characterized for its mechanical properties and the data were used as reference data for the Gr. 91 development program.

**Table 1. Chemical compositions of Gr. 91 plate with heat number 30176 (weight %)**

<b>C</b>	<b>P</b>	<b>Si*</b>	<b>Ni</b>	<b>Mn</b>	<b>N</b>	<b>Ti</b>	<b>Sn</b>	<b>V</b>	<b>Fe</b>	<b>As</b>
0.081	0.010	0.11	0.09	0.37	0.055	0.004	<0.001	0.209	balance	0.001
<b>Zr</b>	<b>S</b>	<b>Cr</b>	<b>Co</b>	<b>Mo</b>	<b>Al</b>	<b>W</b>	<b>Cu</b>	<b>Nb</b>	<b>B</b>	
<0.001	0.003	8.61	0.010	0.89	0.007	<0.01	0.04	0.072	<0.09	

\*Note: heat 30176 is low in Si content.

A photograph of the Gr. 91 plate with heat number 30176 is shown in Fig. 3. This plate was hot forged followed by hot rolling. The nominal thickness of the plate is 1 inch. A section measuring 61" x 25" was cut off from this plate as the supply material for specimen machining. This section of plate material was normalized at 1050°C for one hour and then tempered at 760°C for 2 hours followed by air cooling. The heat treatment was performed by Bodycote Thermal Processing, Inc. in Morristown, Tennessee. The microstructure of the plate was characterized using back scatter electron microscopy (Fig. 4), and it is shown to have typical tempered martensitic features with no untempered martensite. Additional microhardness test results show an average Vickers hardness value of 227 kg/mm<sup>2</sup>, which is within the range of 195-265Hv specified in SA-387. The microstructure analysis and hardness test results confirm that the heat treatment was performed correctly.



**Fig. 3. Gr.91 plate with heat number 30176.**

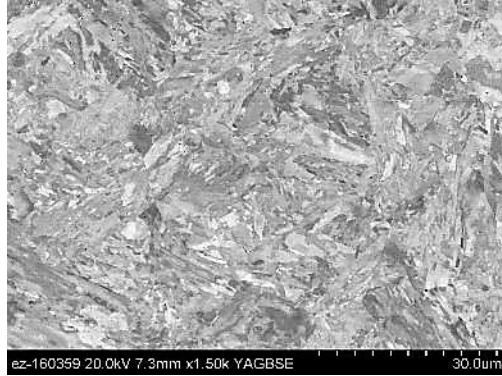


**Fig. 4. Back-scatter image of the Gr. 91 plate (heat 30176) after heat treatment.**

The F91 bar material with nominal 1.25” diameter was purchased from American Alloy Inc. (Houston, Texas). This material was manufactured by BGH Edelstahlwerke GmbH, Freital, Germany. The heat number is 307333 and the as-received F91 bar satisfies ASME SA-182 specification for forging. The chemical composition of the F91 is listed in Table 2. The as-received material was normalized at 1060° C and tempered at 770° C. The microstructure of the F91 bar at the center of the diameter is shown in Fig. 5. The preliminary microstructure analysis shows the martensitic phase is not fully tempered. No significant changes in microstructure were observed along the diameter. Further detailed characterization of the microstructure will be performed, and this material will be heat-treated if necessary. The as-received bar was tested for Vickers microhardness along the diameter, and the results are plotted in Fig. 6 for two line-profiles. The Vickers hardness value was between 209 and 230 kg/mm<sup>2</sup>, within the ASME SA-182 specification. A preliminary SMT experiment on this material was performed on a specimen with as-received condition to compare with the previous SMT tests performed on the Gr. 91 plate (heat 30176).

**Table 2. Chemical compositions of F91 bar material with heat number 307333 (weight %)**

<b>C</b>	<b>P</b>	<b>Si</b>	<b>Ni</b>	<b>Mn</b>	<b>N</b>	<b>Ti</b>	<b>Sn</b>	<b>V</b>	<b>Fe</b>	<b>Nb</b>
0.098	0.019	0.25	0.16	0.44	0.0480	0.002	0.003	0.200	balance	0.079
<b>Zr</b>	<b>S</b>	<b>Cr</b>	<b>Mo</b>	<b>Al</b>						
0.002	0.0020	8.42	0.97	0.002						

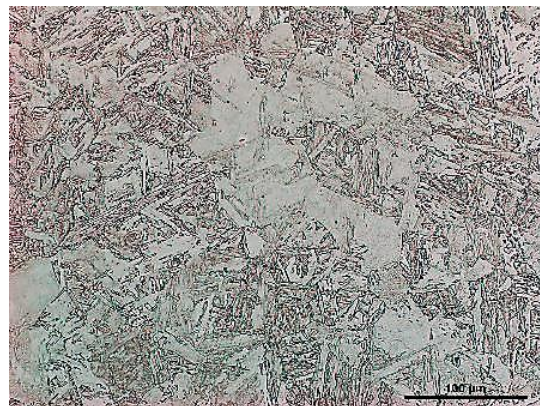


**Fig. 5. Microstructure of the F91 bar material at center line.**

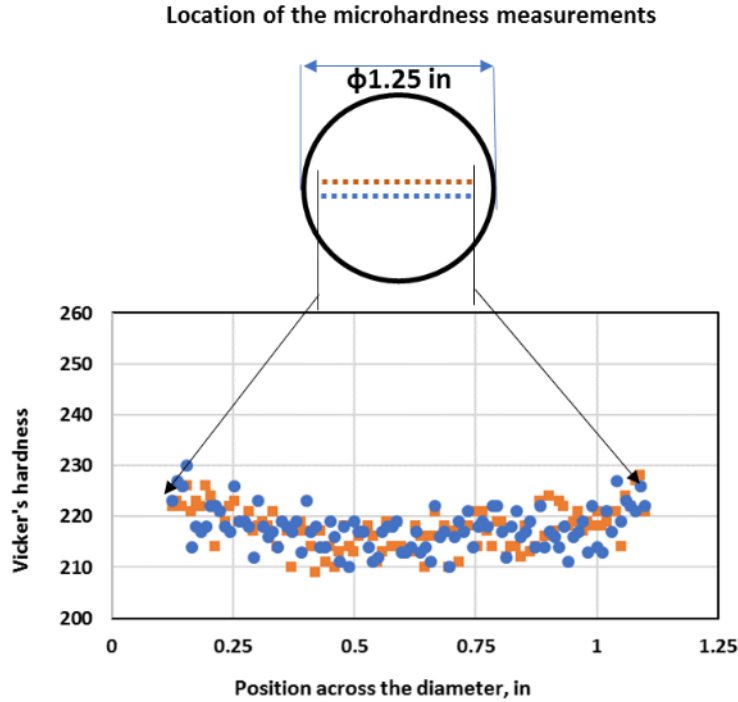


**Fig. 6. Vickers microhardness of the F91 bar material.**

## 2.2 SPECIMENS AND EXPERIMENTS

### 2.2.1 Specimen geometries

Two types of specimen geometries were used in this research. The standard creep-fatigue specimen geometry with 0.25-inch gage diameter is shown in Fig. 7.

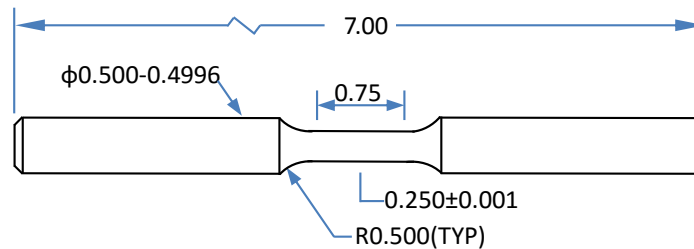


**Fig. 7. Standard creep-fatigue specimen geometry.** Units are in inches.

The combined effect of elastic follow-up and stress concentration is the key principle in SMT specimen design. The Type 1 SMT specimen geometry is shown in Fig. 8. The diameters of the necked test section and the thicker section were designed to have a cross-sectional area ratio of 1:2. The control length for the applied displacement was 5 inches to achieve the designed elastic follow-up. The 0.25-inch transition radius inside the gage section produces a stress intensification factor of 1.37.

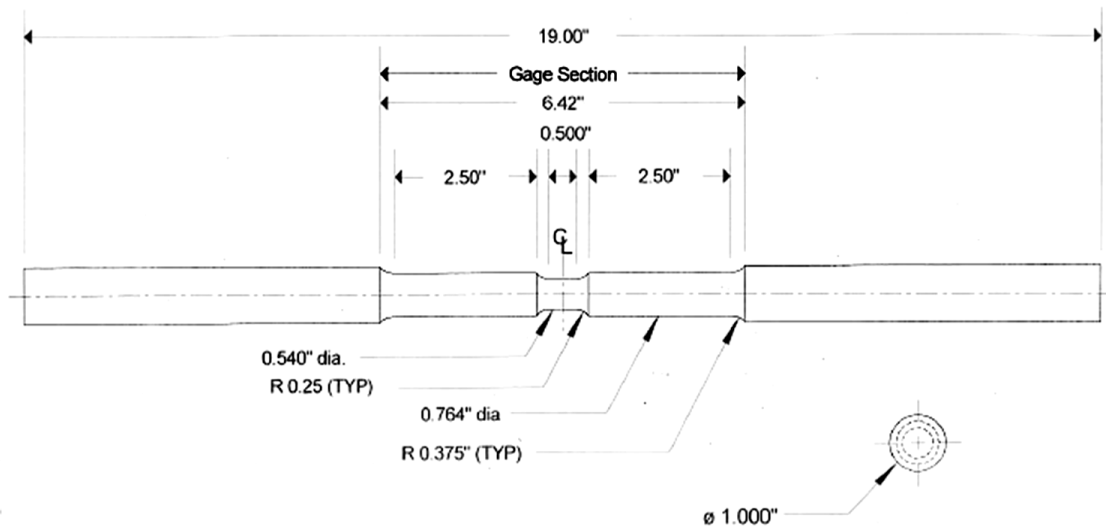


**Fig. 8. Type 1 SMT solid bar specimen geometry.** Units are in inches.

## 2.2.2 Key feature mechanical testing

### 2.2.2.1 Type 1 SMT

Although not a strict requirement for establishing design curves using the SMT approach, strain measurements and the cycles to failure provide insight into the role of elastic follow-up in strain and stress redistribution on cyclic life. In the necked down section of the SMT specimen, there is a 0.5" uniform axial length for local strain measurement with an extensometer of 0.4" gage length. The measured axial strains were used to generate the hysteresis loops along with the applied stresses.

This SMT method requires testing the specimen with accurate end displacement control over a section of the specimen that could result in an effective elastic follow-up. In this study, the end displacement was applied to the controlled total length of 5". The controlled total length includes part of the thicker gage section, the necked test section, and the transition length from the thicker gage section to the necked test section. The accuracy in end displacement control is achieved by testing under strain-control mode using an extensometer with 5" gage length.

Type 1 SMT testing was performed on the newly procured F91 (heat 307333) material with applied compressive end-displacement hold for 10 min at 650° C. The applied end-displacement profile is schematically shown in Fig. 9. The applied end-displacement amplitude was 4.5 mil, corresponding to an elastically calculated strain range of 0.3% in the necked test section.

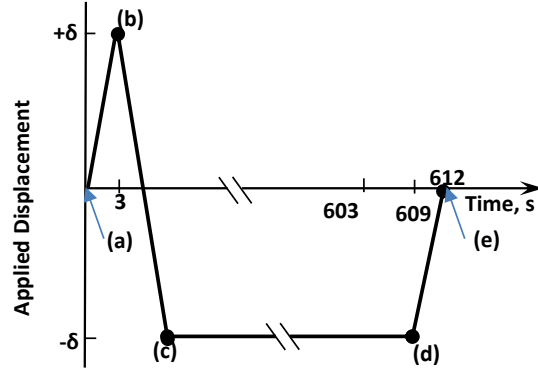


Fig. 9. Applied end-displacement profile for one cycle of SMT creep-fatigue testing compression hold

### 2.2.2.2 Two-bar thermal ratcheting test on Gr. 91

There are two ways to introduce temperature difference in the two bars, i.e., either by introducing a temperature difference at the low temperature end of the thermal cycle or at the high temperature end. Preliminary results using viscoplastic modeling to simulate the two-bar thermal ratcheting system show that the ratcheting rate was faster when the temperature difference was introduced at the low temperature end of the thermal cycle. In order to effectively evaluate the ratcheting behavior experimentally using the two-bar system, it was decided to use the thermal profile shown in Fig. 10 in this study with the time delay introduced between ① and ②. The time delay in the thermal profile defines the temperature difference in the two bars. The thermal strains in the specimens are a function of the time delay, the cooling rate, and the total temperature difference. The heating and cooling rates were  $30^{\circ}\text{C}/\text{min}$ . The equivalent strain rate was calculated to be  $6.5\text{E}-6\text{ s}^{-1}$  from the thermal expansion and the heating/cooling rates. Table 3 summarizes the parameters used for the two-bar experiments and EPP analysis. Experiments were performed on one set of specimens at the temperature range of  $350$  to  $650^{\circ}\text{C}$  with different combinations of total load levels and time delays. The change in loading conditions was performed at  $350^{\circ}\text{C}$  without unloading the specimens to zero load from the previous condition.

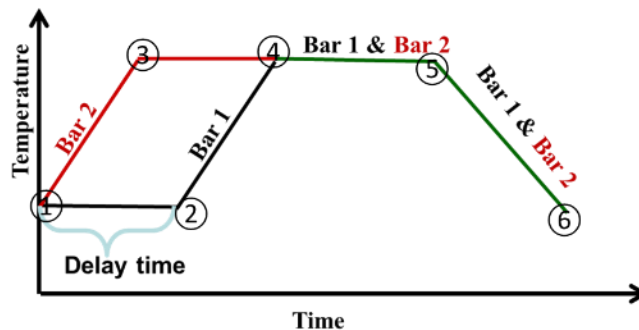


Fig. 10. Two-bar thermal cycle.



**Table 3. Parameters of the two-bar experiment and EPP analysis**

Material	Gr. 91(heat 30176)
Specimen diameter	0.25 in
Temperature range	350 to 650° C
hold time (4) to (5)	60 min
Heating and cooling rate (1) to (3), (2) to (4) and (5) to (6)	30° C/min
time delay, (1) to (2)	From 1 min to 10 min
Applied total load	From -700 to 1,700 lb

Consistent with the preceding work by Wang et al. (2013, 2014, 2015, 2016, 2017), the ratcheting strain is defined as the difference between the mechanical strain at a time point in a thermal cycle and that at the same time point in the reference cycle. When the same point in the thermal cycle is selected, the amount of ratcheting strain calculated based on the total strain is the same as that calculated based on the mechanical strain. In this study, the ratcheting strains were calculated from the maximum total strains of each cycle, and they were approximately the same values as those calculated based on the minimum strains. It was also observed that the cyclic ratcheting rates were approximately constant and the shape of the hysteresis loops were uniform for all the tests conducted after the first several initial cycles. In this study, the ratcheting rates were extrapolated to obtain the ratcheting strain at 350 hours to provide information to our parallel theoretical studies on strain limits of Gr. 91.

### 2.2.3 Mechanical tests to support viscoplastic material model development

Four types of mechanical tests to support viscoplastic material model development were performed to generate results and provide data. All the tests described here were on the plate material (heat 30176) and used the standard specimen geometry shown in Fig. 7.

#### 2.2.3.1 Cyclic stress-strain curves

Cyclic stress-strain curves were generated for temperatures of 21, 260, 371, 427, 482, 538 and 566° C. At each test temperature, a single specimen was cyclic loaded under strain control mode using the multiple step test method. The specimen was sequentially cycled at strain ranges of 0.4%, 1.2%, 2%, 4% and 5% with a fully reversed straining profile (i.e.,  $R=-1$  on applied strain). The specimen was not returned to zero load after testing at the previous strain ranges. There were 19 cycles performed at each strain range (except for the test at 538° C with the strain range of 5%, in which case the specimen failed after 6 cycles of loading). The testing parameters are also summarized in Table 4.

**Table 4. Cyclic stress-strain evaluation of Gr. 91 (heat 30176)**

Material	Gr. 91 (heat 30176)
Specimen diameter	0.25 in
Test Temperatures, °C	21; 260; 371; 427; 482; 538; 566
Strain rate, 1/s	1E-3
Strain ranges, %	0.4; 1.2; 2; 4; 5

#### 2.2.3.2 Sequential creep and strain controlled cycling

The combined sequential creep and fatigue experiment is designed to demonstrate the effect of cyclic loading on creep deformation. The testing procedure is schematically illustrated in Fig. 11. The test

started with a load-controlled creep segment for 24 hours, and then it was unloaded to zero load before switching the test machine to strain-control and cycled for a fatigue segment of 100 cycles. The fatigue segment was at 1% strain range with a  $1\text{E-}3 \text{ s}^{-1}$  strain rate. The sequential creep and fatigue segments were repeatedly applied to the specimen until failure. Tests were performed at two temperatures. The testing parameters are listed below in Table 5.

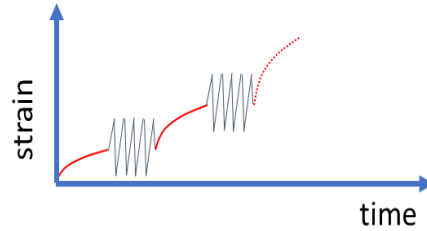


**Fig. 11. Schematics of the combined creep/fatigue experiments.**

**Table 5. Test parameters for combined creep and fatigue experiment on Gr. 91 (heat 30176)**

		Test at 600° C	Test at 550° C
Specimen diameter, in		0.25	0.25
Creep segment	Applied stress, ksi	21.8	34.8
	Loading rate,	1 second to the stress level	1.6 second to the stress level
	Creep segment duration; hrs	24	24
	Total number of creep segments performed before failure	12	4
Fatigue segment	Strain ranges, %	1	1
	Strain rate, 1/s	1E-3	1E-3
	Number of cycles of each fatigue segment	100	100
	Total number of fatigue segments performed before failure	11	3

### 2.2.3.3 Effect of prior strain controlled cycling on strain rate sensitivity

The effect of cyclic softening on strain rate sensitivity was evaluated prior to strain rate jump tests by introducing 150 strain-controlled fatigue cycles at a strain range of 1% and a strain rate of  $1\text{E-}3 \text{ s}^{-1}$  at 600 and 538° C, respectively. The cyclic straining was fully reversed with  $R=-1$  on applied strain. A baseline test was performed on a specimen without any prior cyclic history for comparison purposes. The strain rate jumps were from  $1\text{E-}5$  to  $1\text{E-}4 \text{ s}^{-1}$  at 1% strain, and  $1\text{E-}4$  to  $1\text{E-}3 \text{ s}^{-1}$  at 2% strain. The testing parameters are summarized in Table 6.

**Table 6. Test parameters for rate jump experiment on Gr. 91 (heat 30176)**

Test temperature, °C	600, 538
Specimen diameter, in	0.25
Strain-controlled cycling prior to strain rate jumps	150 cycles, 1% strain range, $1E-3 \text{ s}^{-1}$ , $R=-1$
Initial tensile strain rate, following cycling	$1E-5 \text{ s}^{-1}$
Strain rate jump at 1% strain	$1E-5$ to $1E-4 \text{ s}^{-1}$
Strain rate jump at 2% strain	$1E-4$ to $1E-3 \text{ s}^{-1}$
Experiment control mode,	Strain control

#### 2.2.3.4 Thermal mechanical fatigue

The thermomechanical fatigue experiment was performed at a temperature range of 150 to 650° C with heating and cooling rates of 10° C/min using an igniter heater furnace. The temperature profile was controlled by a LabView program. Prior to the thermomechanical fatigue test, the specimen was thermally cycled at zero load to collect thermal expansion measurement data. Thermomechanical fatigue was induced according to the ASTM-2368-10 standard. It was under strain control with straining cycles that are 180 degrees out-of-phase with the thermal cycles. The total strain was controlled to be zero and the starting temperature was 400° C. The applied strain ratio is -1. The testing parameters are listed in Table 7.

**Table 7. Test parameters for thermomechanical experiment on Gr. 91 (heat 30176)**

Test temperature range	150° C to 650° C
Specimen diameter, inch	0.25
Controlled total strain amplitude	0%
Starting temperature	400° C
Heating and cooling rates	10° C/min
Strain ratio	-1
Temperature mechanical strain phase angle	180 °, i.e., anti-phase thermomechanical fatigue
Experiment control mode	Strain control

### 3. RESULTS AND DISCUSSIONS

#### 3.1 RESULTS FROM KEY FEATURE MECHANICAL TESTING

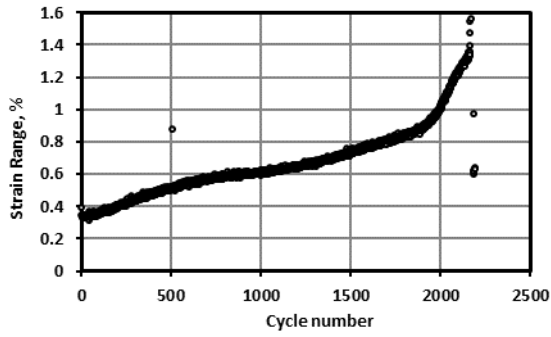
##### 3.1.1 Type 1 SMT Testing

The SMT creep-fatigue test results at 650° C on F91 forged bar Type 1 SMT specimen (heat 307333) are summarized and highlighted in Table 8. Previous Type 1 SMT creep-fatigue evaluation results on the Gr. 91 plate (heat 30176) from Wang et.al. 2016 are also listed for comparison purposes. All tests had the same elastically calculated strain range of 0.3% inside the necked test section. Previous SMT tests performed on Gr. 91 plate (heat 30176) showed that SMT creep-fatigue with compression hold was the most damaging mode. The new SMT test results on F91 forged bar (heat 307333) showed 72% longer SMT creep-fatigue life than the test on Gr. 91 plate (heat 30176), where both were tested under the same loading condition. The measured initial strain range for these two tests was the same.

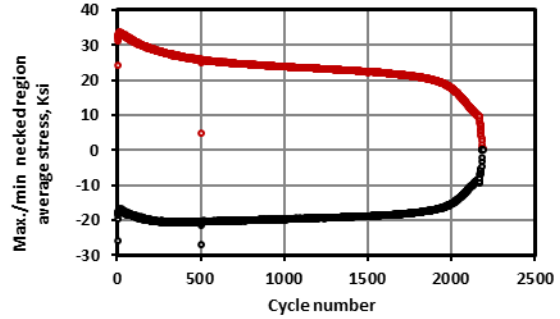
**Table 8. Summary of the SMT creep-fatigue results**

Material	Test No.	Amplitude, $\delta$ value, mil	Elastically calculated strain range inside gage	Hold times (sec)	Loading profile	Initial strain range	Test temperature (° C)	Life time (hrs)	Cycles to failure
Gr. 91 plate (heat 30176)	#28	4.5	0.296%	600	Tension hold	0.37%	650	238	1400
	#29	4.5	0.296%	600	Compression hold	0.33%	650	187	1100
	#30	4.5	0.296%	600	Combined tension and compression hold	0.46%	650	408	1200
F91 bar (heat 307333)	#39	4.5	0.296%	600	Compression hold	0.33%	650	323	1900

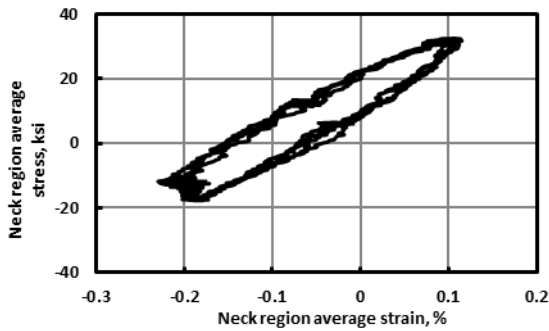
Plots of the measured strain range, maximum (tension) and minimum (compressive) stress as a function of cycles, representative hysteresis loops, stress history and a picture of the failed specimen are shown in Fig. 12. The measured average strain inside the necked test section was shown to ratchet to the tensile direction, and exceeded the 1% strain limit. The measured strain range increased with the increase of the applied cycles, indicating the strong cyclic softening effect. Consistent with the tensile ratcheting behavior, the failed specimen showed necking inside the necked test section.



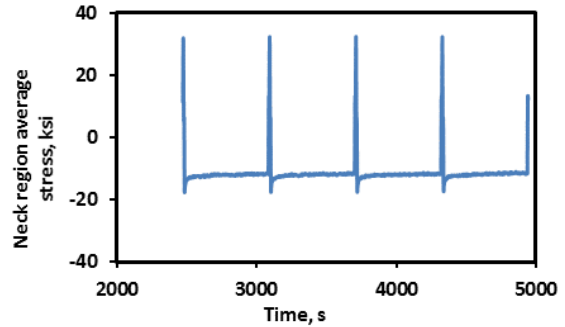
(a) Strain range



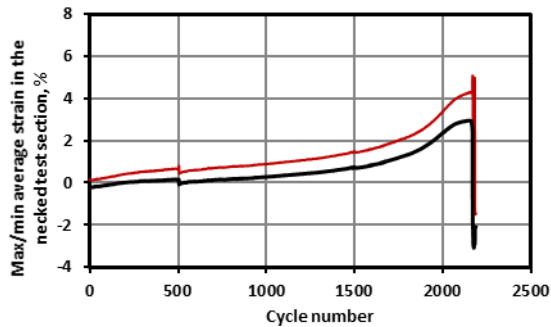
(b) Max/Min stresses



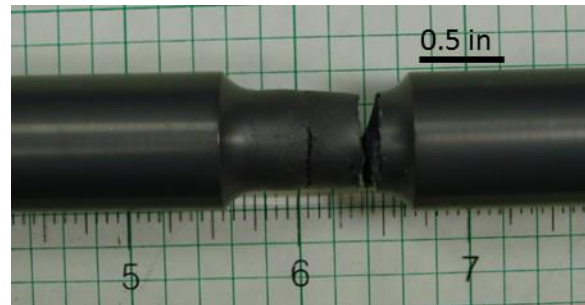
(c) Hysteresis Loop



(d) Stress relaxation at compressive displacement hold



(e) ratcheting strain



(f) failed specimen

**Fig. 12. Test results for test #39-Type 1 SMT on F91 (heat 307333) at 650° C.**

### 3.1.2 Two-bar thermal ratcheting test results

In this reporting period, two-bar thermal ratcheting tests were performed on Gr. 91 plate (heat 30176) to assess the material response to cyclic thermal loading under a two-bar testing condition. The purpose of this test is to establish baseline reference test data for EPP strain limits evaluation. The two bars were thermally cycled between 350 and 650° C using the temperature profile shown in Fig. 10, where Bar 1 had

a time delay in the heating segment. An example of the thermal profile for one cycle is shown in Fig. 13 below for a testing condition with a 10-minute time delay.

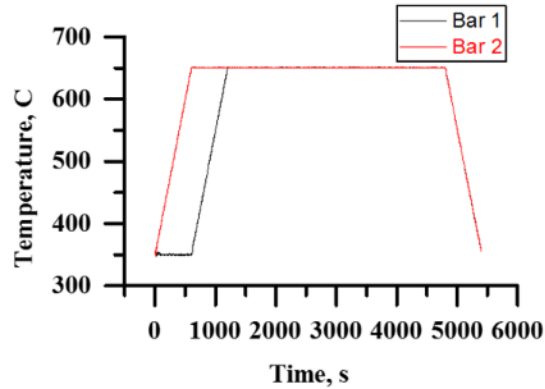


**Fig. 13. An example of the thermal profile with 10 mins. time delay.**

The thermal ratcheting tests at different applied mean stress and time delay were performed on the same two bars with sequential test numbers of T30-1 to T30-10. The test parameters and results for these testing conditions are summarized in Table 9. Note that the first 10 cycles on the first test, T30-1, were not stable, the values given in Table 9 were based on cycle No. 11 to 34, while the values of the remaining nine test conditions were based on all the available cycles.

**Table 9. Summary of the two-bar thermal ratcheting experiments on Gr. 91 (heat 30176)  
for temperature range of 350 to 650° C.**

<i>Test No.</i>	<i>T30-1</i>	<i>T30-2</i>	<i>T30-3</i>	<i>T30-4</i>	<i>T30-5</i>
Applied mean stress, MPa	-7.5±0.7 (cycle No.11-34)	49.4 ±0.7 (All cycles)	63.7±2.6 (All cycles)	80.8±0.6 (All cycles)	98.4±0.7 (All cycles)
Time delay (minutes)	10	10	10	10	10
Nominal total load (pounds)	-100	700	900	1150	1400
Total number of cycles tested	34	45	35	33	32
Ratcheting rate (per cycle), %	-0.0045	-2E-5	9E-4	0.0015	0.006
Initial stress on Bar 1, MPa	-13	-58.6	-0.075	28.9	64.9
Initial stress on Bar 2, MPa	-12	155.6	126.8	132.8	132.6
Initial residual total strain, %	0	-0.37	-0.37	-0.2	-0.1
Reference cycle No.	11	10	10	10	10
Reference cycle minimum total strain, %	-0.3	-0.28	-0.25	-0.17	-0.013
Stress range per cycle for Bar 1, MPa	283±3.3 (cycle No.11-34)	286.9±1.2	287.5±1.4	285.7±1.0	285.9±1.4
Stress range per cycle for Bar 2, MPa	277±3.0 (cycle No.11-34)	282.9±1.0	283.8±2.5	284.0±1.6	283.7±1.3

<i>Test No.</i>	<i>T30-6</i>	<i>T30-7</i>	<i>T30-8</i>	<i>T30-9</i>	<i>T30-10</i>
Applied mean stress, MPa	-28.3±0.8 (All cycles)	119.8±0.8 (All cycles)	-28.3±0.8 (All cycles)	-50.0±0.7 (All cycles)	119.3±0.8 (All cycles)
Time delay, min	10	8	6	5	3
Nominal total load, lbs	-400	1700	-400	-700	1700
Total number of cycles tested	32	15	33	35	30
Ratcheting rate (per cycle), %	-0.026	0.11	0.0027	-0.0035	0.09
Initial stress on Bar 1, MPa	-47	3.1	-47.1	-131.5	58.1
Initial stress on Bar 2, MPa	-10.9	234.7	-10.9	31.6	181.6
Initial residual total strain, %	0.087	-1.055	0.76	0.35	0.28
Reference cycle No.	10	1	10	10	10
Reference cycle minimum total strain, %	-0.492	-1.056	0.45	0.28	1.17
Stress range per cycle for Bar 1, MPa	284.2±4.0	267.1±2.9	202.8±7.9	166.5±1.5	98.7±1.8
Stress range per cycle for Bar 2, MPa	281.8±4.3	264.4±6.1	200.2±8.4	164.7±3.7	95.4±3.5

Table 10 summarizes the results on strain limits evaluation for the 10 experimental loading conditions. The EPP strain limits evaluation followed the procedure in ASME B&PV Code Case N-861, and the details are also described in Messner and Sham, 2017. Note that the EPP evaluation in this table used the pseudo-yield stress from the isochronous curves of Gr. 91 in the ASME design code, which do not capture any effect from prior cyclic softening history. There is on-going research effort in modifying the EPP Code Cases for Gr. 91 to take into consideration the cyclic softening effect (Messner and Sham, 2017). Comparison of the experimental results and the un-modified EPP strain limits evaluation shows there are no measured strains greater than 1% that pass the EPP checks. There are two experimental points (-400 lb total load with 6 min delay and -700 lb total load with 5 min delay) that exceed 1% ratchet strain in 350 hours, but they failed the EPP strain limits evaluation, thus demonstrating the conservatism of the (unmodified) EPP strain limits procedure.

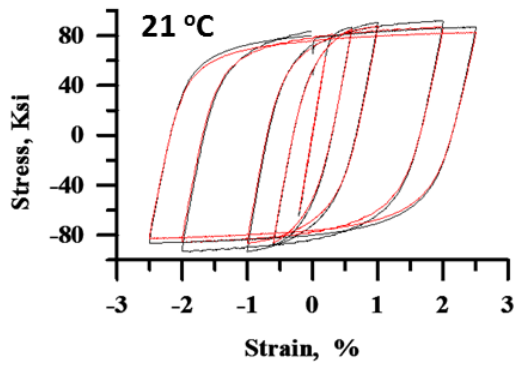
**Table 10. Two-bar thermal ratcheting results on Gr. 91 (heat 30176) with 350 hr extrapolation.**

Applied total load, lbs	Time Delay, min	Test < 1% ?	Unmodified EPP < 1% ?
-100	10	No	No
700	10	Yes	Yes
900	10	Yes	Yes
1150	10	Yes	Yes
1400	10	No	No
-400	10	No	No
1700	8	No	No
-400	6	Yes	No
-700	5	Yes	No
1700	3	No	No

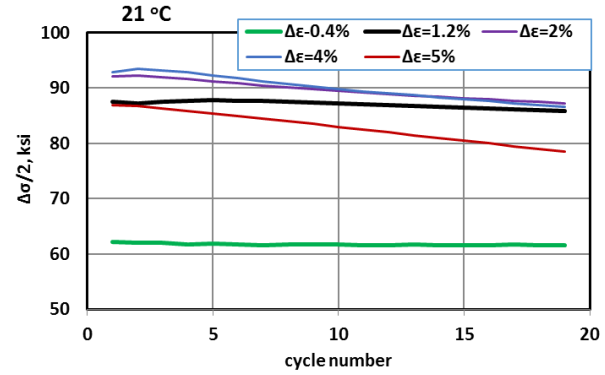
### 3.2 RESULTS FROM MECHANICAL TESTS IN SUPPORT OF VISCOPLASTIC MATERIAL MODEL DEVELOPMENT

#### 3.2.1 Cyclic stress-strain curves

Cyclic stress-strain curves for Gr. 91 (heat 30176) generated at temperatures of 21, 260, 371, 427, 482, 538 and 566° C are plotted in Fig. 14 to Fig. 20. Only the first cycle and the last cycle at each strain ranges are shown in these plots. The stress amplitude as a function of the applied cycles is also shown in these figures. The results reveal the material had cyclic softening behavior at all temperatures at strain ranges of 2%, 4% and 5%. No significantly cyclic softening was observed for the tested cycles at 0.4% strain range at all temperatures, indicated by the constant stress amplitude as a function of the applied testing cycles. At temperatures of 21, 260, 371 and 427° C, the cyclic softening rate increases when the strain ranges are increased, shown as the increasing slopes of the stress amplitude as a function of the applied cycles. For test temperature of 482, 538 and 566° C, the cyclic softening rate is similar for the available cycles at the strain ranges of 1.2% and higher.

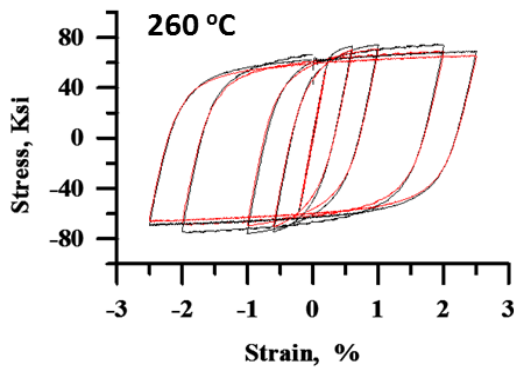


(a) Cyclic stress strain curve

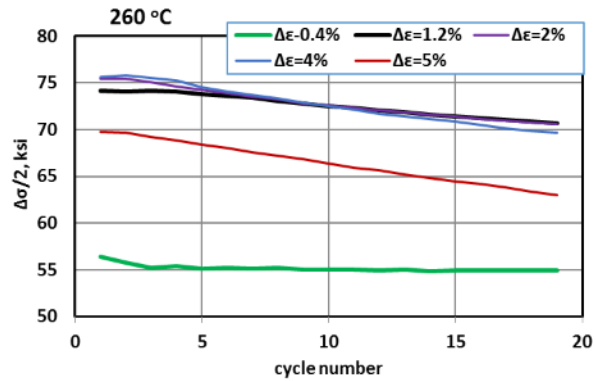


(b) Stress amplitude vs cycle number

**Fig. 14. Cyclic stress-strain evaluation of Gr. 91 (heat 30176) at 21° C.** Black lines are the first cycles and red lines are the last cycles.

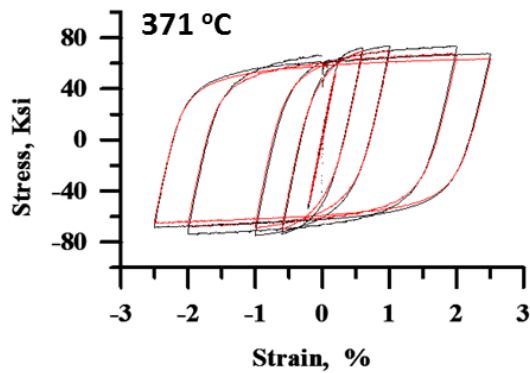


(c) Cyclic stress strain curve

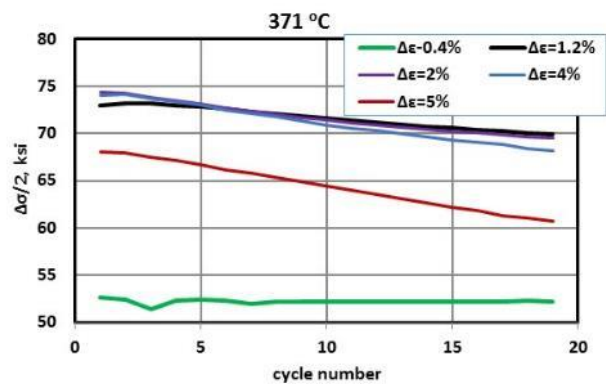


(d) Stress amplitude vs cycle number

**Fig. 15. Cyclic stress-strain evaluation of Gr. 91 (heat 30176) at 260° C.** Black lines are the first cycles and red lines are the last cycles.

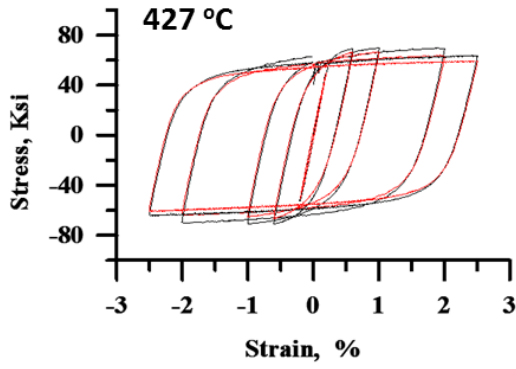


(a) Cyclic stress strain curve

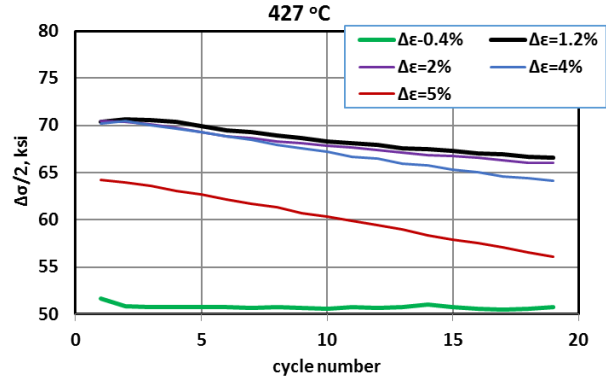


(b) Stress amplitude vs cycle number

**Fig. 16. Cyclic stress-strain evaluation of Gr. 91 (heat 30176) at 371° C.** Black lines are the first cycles and red lines are the last cycles.

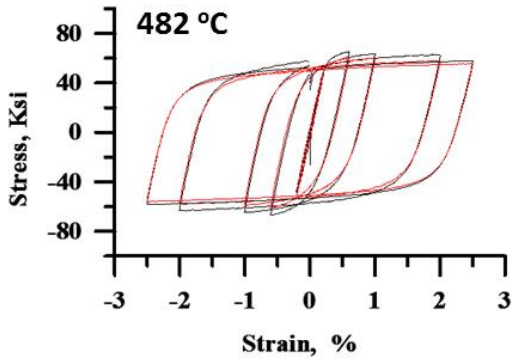


(a) Cyclic stress strain curve

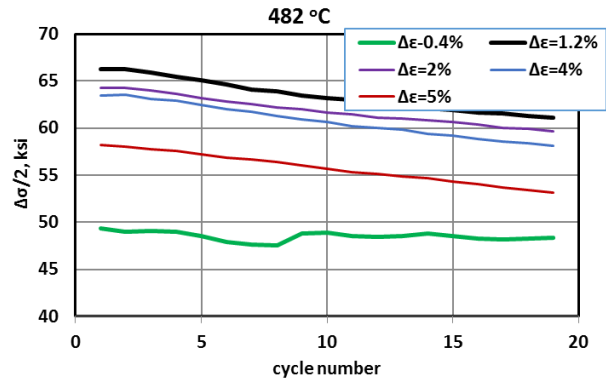


(b) Stress amplitude vs cycle number

Fig. 17. Cyclic stress-strain evaluation of Gr. 91 (heat 30176) at 427° C. Black lines are the first cycles and red lines are the last cycles.

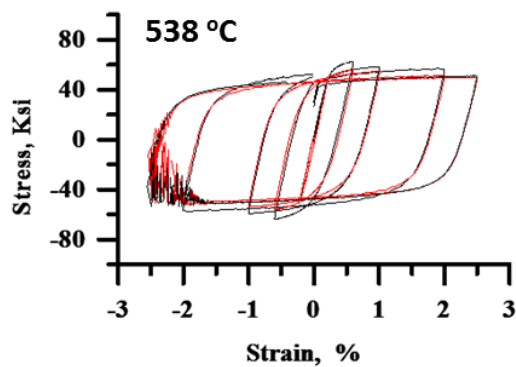


(a) Cyclic stress strain curve

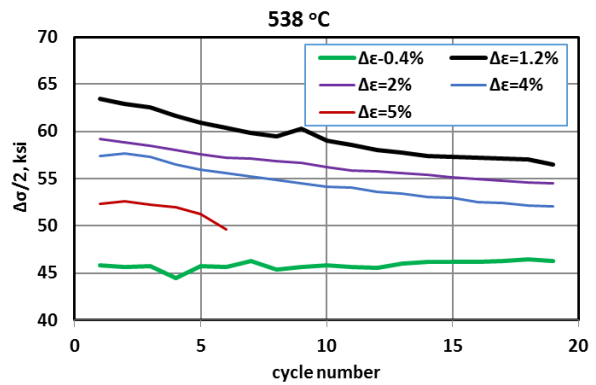


(b) Stress amplitude vs cycle number

Fig. 18. Cyclic stress-strain evaluation of Gr. 91 (heat 30176) at 482° C. Black lines are the first cycles and red lines are the last cycles.



(a) Cyclic stress strain curve



(b) Stress amplitude vs cycle number

Fig. 19. Cyclic stress-strain evaluation of Gr. 91 (heat 30176) at 538° C. Black lines are the first cycles and red lines are the last cycles.

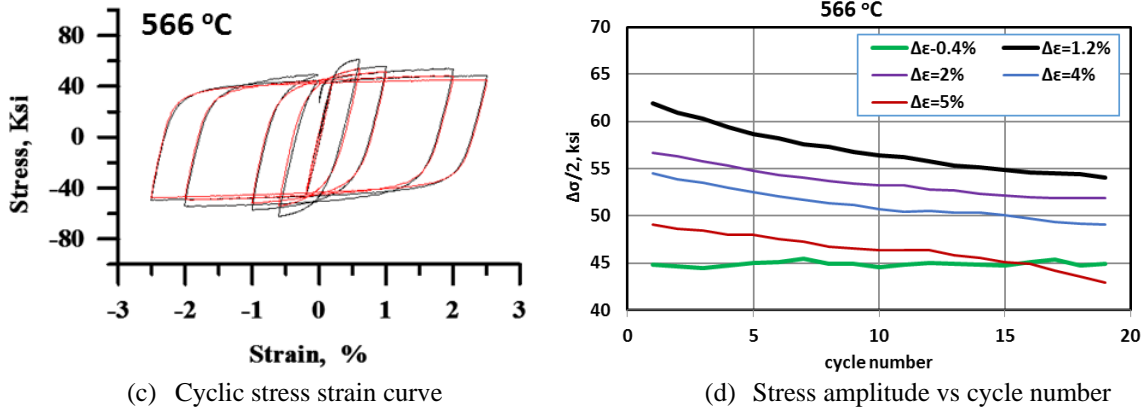


Fig. 20. Cyclic stress-strain evaluation of Gr. 91 (heat 30176) at 566° C. Black lines are the first cycles and red lines are the last cycles.

### 3.2.2 Sequential creep and strain controlled cycling

The effect of cyclic softening on creep rate is evaluated by introducing into a creep test strain-controlled cyclic fatigue segments of 100 cycles at 1% strain range every 24 hours. These types of tests can establish reduction factors to adjust the existing ASME Code isochronous curves for Gr. 91 to account for cyclic softening (see Messner and Sham, 2017). Softened isochronous data may be needed to preserve the conservatism of the EPP methods for fatigue-dominated load histories. Here the preliminary test results at two selected temperatures are reported. The test results at 600° C are shown in Fig. 22, with (a) the collection of the creep curves from all the creep segments, (b) the minimum creep rates for each creep segment at 150 MPa (21.8 ksi) stress, and (c) the maximum/minimum stresses from all the fatigue segments. Creep curve at slightly higher stress of 160 MPa by Kimura et. al. 2009 is compared in (a) and the corresponding creep rates at 24-hour intervals are shown in Fig. 22b. The results show that introduction of fatigue segments increased the creep rates significantly and shortened creep life. However, the addition of creep segments did not affect its fatigue life under this test condition.

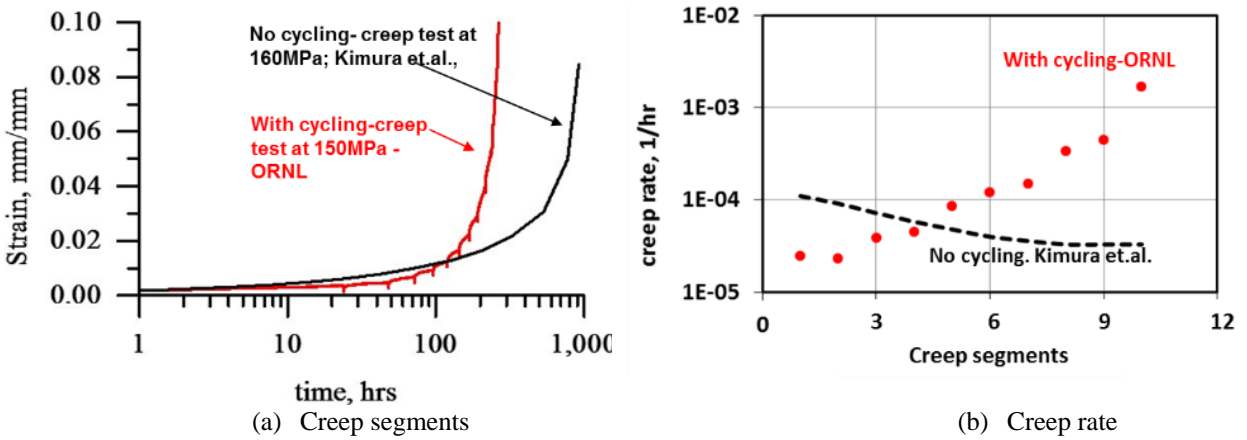


Fig. 21. Combined creep-fatigue test on Gr. 91 (heat 30176) at 600o C. (continued on next page)

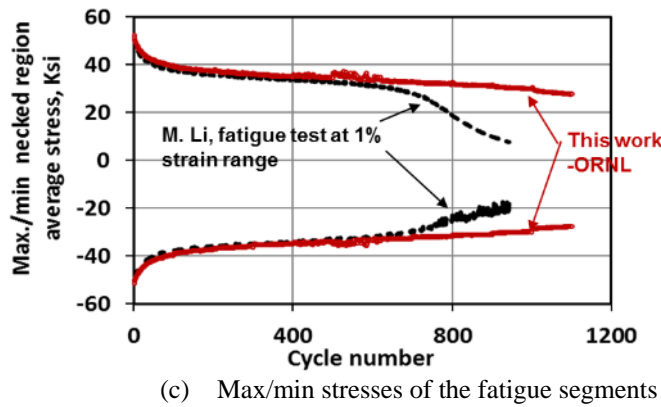


Fig. 22. Combined creep-fatigue test on Gr. 91 (heat 30176) at 600° C.

The test results for a combined creep and fatigue experiment at 550° C are shown in Fig. 23. Tests included repeating 24-hour creep segments at 240MPa combined with 100 cycles of fatigue segments. The results show creep rates increased by two orders of magnitude due to the addition of the fatigue segments after four repeats. Under this test condition, the addition of creep segments decreased fatigue life by 60%.

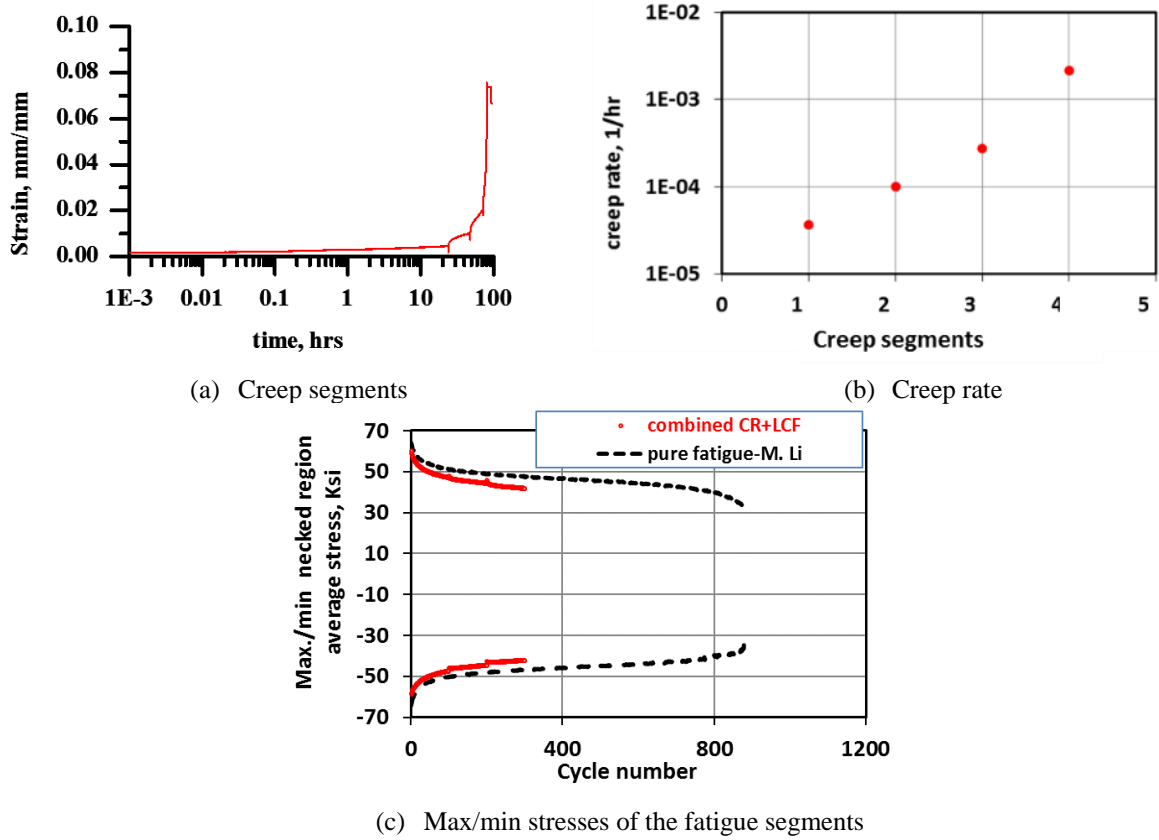


Fig. 23. Combined creep-fatigue test on Gr. 91 (heat 30176) at 550° C.

### 3.2.3 Effect of prior strain controlled cycling on strain rate sensitivity

The effect of cyclic loading on strain rate sensitivity was evaluated at 600° C and 538° C. The true stress-true strain curves for a test with 150 cycles of fatigue loading with 1% strain range are plotted in Fig. 24. The true stress-strain curves of the specimen without any cyclic loading history are also shown in the plots for comparison. At both temperatures, the material showed decreased strain rate sensitivity with prior cyclic softening. The 600° C data showed higher strain rate sensitivity than the 538° C data.

Strain rate sensitivity is also evaluated quantitatively using the strain rate sensitivity exponent. The strain rate sensitivity exponent,  $m$ , is defined as:

$$m = \frac{\log(\sigma_2) - \log(\sigma_1)}{\log(\dot{\epsilon}_2) - \log(\dot{\epsilon}_1)} \quad (1)$$

where,  $\sigma_1$  and  $\sigma_2$  are the true stresses before and after rate jump, and  $\dot{\epsilon}_1$  and  $\dot{\epsilon}_2$  are the strain rates before and after rate jump. The  $m$  values are summarized in Table 11. The reduced strain rate sensitivity is demonstrated by the decreased  $m$  values.

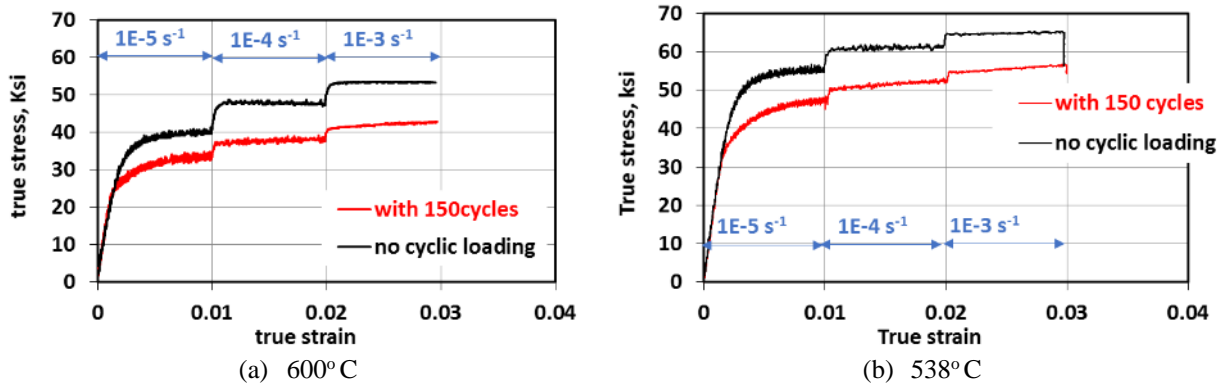


Fig. 24. Effect of cyclic softening on strain rate sensitivity.

Table 11. Effect of cyclic softening on strain rate sensitivity

Test condition		<i>m</i> value of rate jump at 1% strain	<i>m</i> value of rate jump at 2% strain
Test temperature 600°C	Without cyclic loading history	7.9E-2	4.6E-2
	With 150 cycles loading history	4.3E-2	3.3E-2
Test temperature 538°C	Without cyclic loading history	3.8E-2	2.2E-2
	With 150 cycles loading history	2.5E-2	1.5E-2

### 3.2.4 Thermomechanical fatigue

The thermal expansion coefficient was determined to be  $13.1E-6$  in/in/ $^{\circ}$ C using a linear fit of the free expansion curves, as shown in Fig. 25. The mechanical strain is calculated by subtracting the thermal expansion from the total strain. The strain range for this test was 0.65%. The strain rate was determined by the heating and cooling rate, and it was  $2.2E-6$  s $^{-1}$ . The thermal cycle profile, mechanical strain history, representative hysteresis loops, and the maximum and minimum stresses are plotted in Fig. 26. The specimen was tested for 215 cycles and did not fail at end of the test. The absolute values of the maximum stress are higher than those of the minimum stresses due to the fact that the maximum stress was the material response at the lowest temperature of 150°C in the cycle, while the minimum stress was at the highest temperature 650°C, which is also the reason that the minimum stresses saturated much faster than the maximum stress as a function of applied cycles. The cyclic softening effect is also evidently shown from the hysteresis loops.

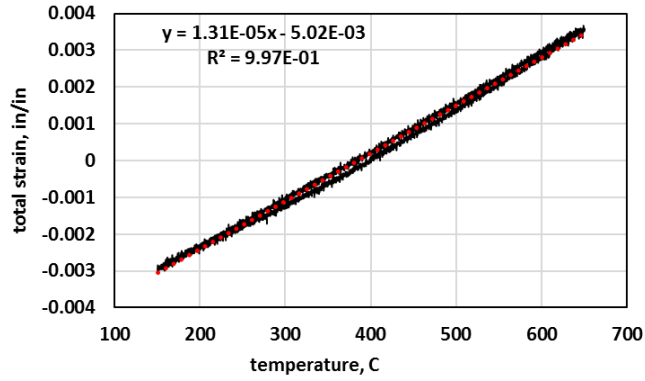
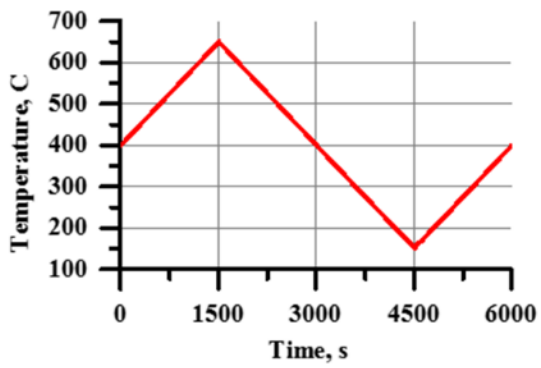
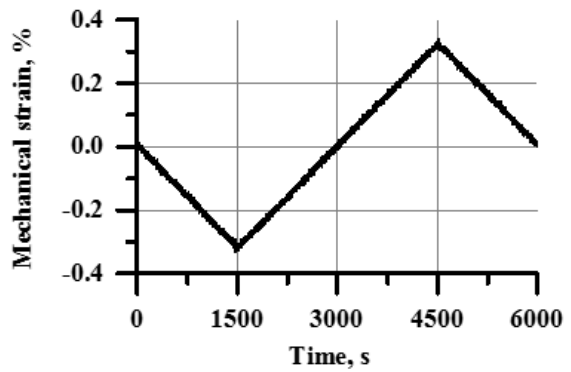


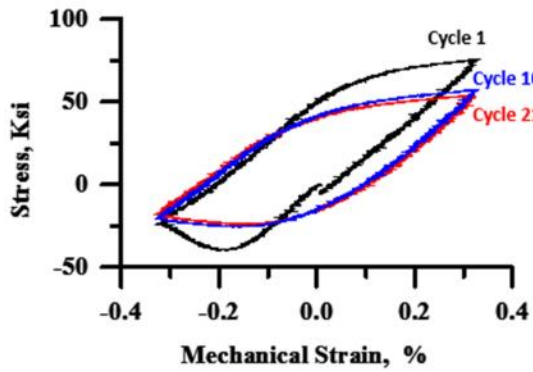
Fig. 25. Thermal expansion measurement (Gr. 91 heat 37016)



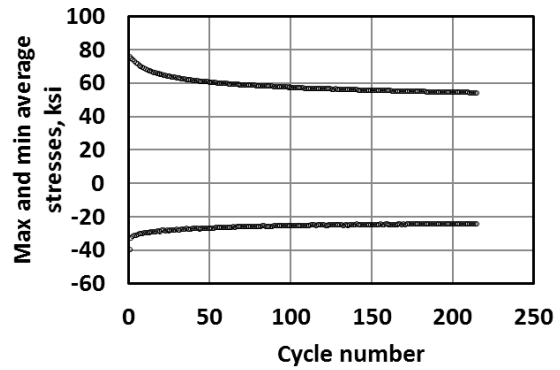
(a) Thermal cycle



(b) Mechanical strain



(c) Hysteresis loops



(d) Maximum and minimum stresses

Fig. 26. Thermo-mechanical fatigue at temperature range of 150 to 650° C.

#### 4. SUMMARY

Key feature tests using the Simplified Model Test (SMT) and two-bar thermal ratcheting approaches have been initiated to both qualify the Elastic – Perfectly Plastic (EPP) design methodologies for Gr. 91 and also to support incorporation of these design rules for Gr. 91 into the ASME Division 5 Code. SMT is an alternative approach to determine cyclic life at elevated temperature, and it avoids parsing the damage into creep and fatigue components. Preliminary testing on Type 1 SMT was performed at 650° C with compression hold on a newly procured F91 forged bar (heat 307333), and it demonstrated 72% longer cycle life than the results from the Gr 91 plate (heat 30176). Two-bar thermal ratcheting behavior of Gr. 91 was evaluated at temperatures ranging from 350 to 650° C using the plate heat. The results were compared with EPP strain limits analysis and verified the conservative nature of that methodology. Experiments were designed and performed to evaluate the effect of cyclic softening, with results showing that cyclic loading history increases creep rate and decreases strain rate sensitivity. In addition, cyclic stress-strain curves were generated and thermomechanical test were performed to provide experimental data to calibrate the viscoplastic material model.

## REFERENCES

1. ASME B&PV Code Case N-861 “Satisfaction of Strain Limits for Division 5 Class A Components at Elevated Temperature Service Using Elastic-Perfectly Plastic Analysis”.
2. ASME B&PV Code Case N-862 “Calculation of Creep-Fatigue for Division 5 Class A Components at Elevated Temperature Service Using Elastic-Perfectly Plastic Analysis Section III, Division 5”.
3. Jetter, R. I., 1998, *An Alternate Approach to Evaluation of Creep-Fatigue Damage for High Temperature Structural Design*, Vol. 5, American Society of Mechanical Engineers, New York, pp. 199–205.
4. J. R. DiStefano et al., (1985), *Summary of Modified 9Cr-1Mo Steel Development Program: 1975-1985*, Technical Report No. ORNL-6303, Oak Ridge National Laboratory, Oak Ridge, Tennessee.
5. K. Kimura, H. Kushima, and K. Sawada (2009), “Long-term creep deformation property of modified 9Cr-1Mo steel,” *Materials Science and Engineering A*, 510-511(C):58–63.
6. Messner, M. C. and Sham, T.-L., (2017), *FY17 Status Report on the Initial EPP Finite Element Analysis of Grade 91 Steel*, Technical Report No. ANL-ART-94, Argonne National Laboratory, Chicago, IL.
7. Swindeman, R., Robinson, D., Williams, B. and Thomas, D., (1982), *Two-Bar Thermal Ratcheting Experiments on 2¼Cr-1Mo Steel*, Technical Report No. ORNL/TM-8001, Oak Ridge National Laboratory, Oak Ridge, TN.
8. Wang, Y., Sham, T.-L., and Jetter, R. I., (2013), *Progress report on the development of test procedure for the two-bar thermal ratcheting experiment for Alloy 617*, ORNL/TM-2013/318, Oak Ridge National Laboratory, Oak Ridge, TN.
9. Wang, Y., Jetter, R. I. and Sham, T.-L., (2014), *Application of Combined Sustained and Cyclic Loading Test Results to Alloy 617 Elevated Temperature Design Criteria*, ORNL/TM-2014/294, Oak Ridge National Laboratory, Oak Ridge, TN.
10. Wang, Y., Jetter, R. I., Baird, S. T., Pu, C. and Sham, T.-L., (2015), *Report on FY15 Two-Bar Thermal Ratcheting Test Results*, ORNL/TM-2015/284, Oak Ridge National Laboratory, Oak Ridge, TN.
11. Wang, Y., Jetter, R. I., and Sham, T.-L., (2016), *Preliminary Test Results in Support of Integrated EPP and SMT Design Methods Development*, ORNL/TM-2016/76, Oak Ridge National Laboratory, Oak Ridge, TN.
12. Wang, Y., Jetter, R. I., Messner, M., Mohanty, S., and Sham, T.-L., (2017), “Combined Load and Displacement Controlled Testing to Support Development of Simplified Component Design Rules for Elevated Temperature Service”, *Proceedings of the ASME 2017 Pressure Vessels and Piping Conference*, PVP2017-65455.

## ELECTRONIC DISTRIBUTION

<b>Name</b>	<b>Affiliation</b>	<b>Email</b>
Corwin, W.	DOE-NE	william.corwin@nuclear.energy.gov
Sowinski, T. E..	DOE	thomas.sowinski@nuclear.energy.gov
Grandy, C.	ANL	cgrandy@anl.gov
Hill, R.N.	ANL	bobhill@anl.gov
Jetter, R.I.	R.I. Jetter Consulting	bjetter@sbcglobal.net
Lara-Curzio, E.	ORNL	laracurzioe@ornl.gov
Li, M.	ANL	mli@anl.gov
Lin, L.	ORNL	linl@ornl.gov
McMurtrey, M.	INL	michael.mcmurtrey@inl.gov
Messner, M.C.	ANL	messner@anl.gov
Sham, T.-L.	ANL	ssham@anl.gov
Wang, H.	ORNL	wangh@ornl.gov
Wang, Y.	ORNL	wangy3@ornl.gov
Wright, R.N.	INL	richard.wright@inl.gov